Journal of Solid State Chemistry 184 (2011) 419–426

Contents lists available at ScienceDirect

Journal of Solid State Chemistry

journal homepage: www.elsevier.com/locate/jssc

Assembly of two layered cobalt–molybdenum phosphates: Changing interlayer distances by tuning the lengths of amine ligands

Yu-Nan Zhang [a,c], Bai-Bin Zhou [a,b,*], Jing-Quan Sha [c], Zhan-Hua Su [b], Ji-Wen Cui [c]

[a] School of Chemical Engineering, Harbin Institute of Technology, Harbin 150001, PR China
[b] Key Laboratory of Materials Physics and Chemistry, Colleges of Heilongjiang Province, School of Chemistry and Chemical Engineering , Harbin Normal University, Harbin 150025, PR China
[c] College of Pharmacy, Jiamusi University, Jiamusi 154007, PR China

ARTICLE INFO

Article history:
Received 8 September 2010
Received in revised form
20 November 2010
Accepted 5 December 2010
Available online 17 December 2010

Keywords:
Cobalt–molybdenum phosphates
Two layered framework
Hydrothermal synthesis
Magnetic property

ABSTRACT

By using amines with different lengths, two layered cobalt–molybdenum phosphates with different interlayer distances, $(C_2N_2H_{10})$ $[HCo(H_2O)_2P_2MoO_{10}]$ **(1)**, and $(C_3N_2H_{12})_4\{Co_3$ $[P_4Mo_6O_{26}(OH)_5]_2\}\cdot 5H_2O$ **(2)**, have been hydrothermally synthesized and characterized. In compound **1**, the H_2en direct the $[CoMoP_2]$ clusters to form a layered framework. By changing the lengths of protonated organic amines (H_2en to 1, 3-H_2pn), compound **2** is obtained, in which the sandwich-shaped $[Co(Mo_6P_4)_2]$ clusters are linked by tetrahedrally coordinated cobalt into a layered framework. With the lengths of protonated organic amines increasing, the interlayer distances in compound **2** become larger. This work successfully demonstrates that tuning the lengths and conformation of the protonated organic amines can provide a facile route for the formation of organically templated inorganic open-framework materials. Additionally, susceptibility measurement shows that the two compounds both exhibit antiferromagnetic interactions.

1. Introduction

The desire to control morphology and size of inorganic frameworks on molecular length scales has led to the design of architectures with complexities extending beyond the molecule. The prospect of creating new functional materials with tunable structures provides a great motivation for research on open-frameworks [1–3]. Open-framework structures exhibited many fascinating structural features and widespread applications in catalysis, separation processes, and magnetic materials [4–10]. Polyoxometalates (POMs), as one kind of well-known metal oxide clusters with nucleophilic oxygen-enriched surfaces and abundant topologies, can be viewed as one kind of inorganic building blocks for constructing multi-dimensional open-framework materials [11–14]. So the syntheses of multi-dimensional open-framework materials based on POMs are very significant. Usually, a promising tool for these materials' design is the evaluation and use of templates under hydrothermal conditions [15–18]. As a smart structure-directing agent, organic amines could exert the template role to direct the construction of novel structures with layered or channel-like frameworks during the self-assembly of POM-based open-frameworks [19–23]. However, the structure-directing effect of organic amines is not restricted to the formation of conceived frameworks. Although the structure directing effect of the organic amines has been studied in detail, the role of amines used in open-frameworks synthesis is not clear and certainly bears further investigation [24]. Therefore, it remains a formidable challenge to rationally control the shape and/or size of a specific framework with affecting its geometrical characteristics.

In the reported works, some researchers have discussed the influences of organic amines on the structures of POM-based compounds. Cronin's group reported the use of rigid organic amines to isolate new cluster types by virtue of the cations used to 'encapsulate' the new building blocks [25–29]. By trapping clusters during the self-assembly process it may be possible to restrain the cluster from reorganizing into other well-known structure types [20]. More recently, Xia's group and co-wokers have discussed influence of the steric hindrance of organic amines and pH values on the supramolecular network based on polyoxomolybdates with transition-metal complexes (PMo–TMCs) [30,31]. In fact, we have recently investigated the effect of amines in the crystal engineering of PMo–TMCs under hydrothermal conditions and found that existence of protonated organic amines can induce the formations of the lacunary wheel-type polyoxoanions and the 3D inorganic open-framework during the self-assembly process [32,33]. Further, preliminary data do imply that the geometry, rigidity and hydrogen bonding ability of the organic amine can influence the overall structure of the framework. More importantly we realized that the presence of the organic amine

* Corresponding author at: School of Chemical Engineering, Harbin Institute of Technology, Harbin 150001, PR China. Tel.: +86 451 88060770.
E-mail addresses: zhangyunan79@163.com (Y.-N. Zhang), bbzhou@hrbnu.edu.cn, zhou_bai_bin@163.com (B.-B. Zhou).

0022-4596/$ - see front matter © 2010 Elsevier Inc. All rights reserved.
doi:10.1016/j.jssc.2010.12.010

might significantly affect the size of the inner space in the framework. Therefore, variation of the size or shape of the organic amine was envisaged to resize the inner space in the framework.

Hence, a motivation for design an appealing route to resize the inner space of the inorganic framework of PMo–TMCs by tuning the lengths of organic amines under hydrothermal conditions has been put forward. In our ongoing research to explore the possible effect of organic amines in the crystal engineering of PMo–TMCs, we have chosen aliphatic amines possessing different lengths, ethylenediamine(en) and 1,3-propanediamine(pn). The following points are taken into consideration: (1) when summarizing the organic amine templated PMo–TMCs, we found that the open-framework directed by protonated aliphatic amines, such as ethylenediamine, were usually regular [19–23,25–29]. (2) The H_2en and H_2pn ligands possess the same type of two terminal amino groups but different spacer. (3) In contrast with H_2en, the –(CH_2)– part of the H_2pn can provide a more flexible role in the crystal engineering of PMo–TMCs. As a result, two layered cobalt–molybdenum phosphates with different interlayer distances were obtained, $(C_2N_2H_{10})$ $[HCo(H_2O)_2P_2MoO_{10}]$ **(1)** and $(C_3N_2H_{12})_4$ $[Co_3$ $[P_4Mo_6O_{26}(OH)_5]_2]\cdot 5H_2O$ **(2)**. Compounds **1** and **2** represent layered frameworks to accommodate H_2en and H_2pn templates, respectively, thus furnishing a unique example in which the interlayer distances of layered framework that can be adjusted by changing the lengths of amine ligands.

2. Experimental

2.1. Materials and methods

All chemicals were purchased commercially and used without further purification. Elemental analyses were performed on a PE2400 SERIES II (CHNSO) Elemental Analyzer. IR spectra were recorded in the range of 400–4000 cm^{-1} on a Nicolet Impact 410 FT/IR spectrometer with pressed KBr pellets. Thermogravimetric analyses were recorded in a dynamic nitrogen atmosphere with a heating rate of 10 °C/min using a Mettler TGA/SDTA851e thermal analyzer. Magnetic susceptibility data were collected over the temperature range of 2–300 K in a magnetic field of 1000 Oe on a Quantum Design MPMS-5 SQUID magnetometer.

2.2. Synthesis of $(C_2N_2H_{10})[HCo(H_2O)_2P_2MoO_{10}]$ (**1**)

A mixture of $Na_2MoO_4\cdot 2H_2O$ (1.452 g), $2CoCO_3\cdot 3Co(OH)_2\cdot H_2O$ (0.48 g), ethylenediamine tetraacetic acid (EDTA) (0.744 g), H_3PO_4 (2 mL, 85%), ethylenediamine (0.5 mL) was dissolved in 30 mL of water. The mixture was stirred for 2 h at room temperature and then heated in a 50 mL Teflon-lined stainless steel autoclave for 7 days at 180 °C. After slow cooling to room temperature, the solid product containing pink block shaped crystals were isolated in 29% yield (based on Co). Anal. Found (%): C, 5.33; H, 3.55; N, 5.51. Calcd. (%): C, 5.05; H, 3.18; N, 5.89. IR (KBr, pellet): 3510 (m), 1632 (m), 1521 (m), 1526 (m), 1471 (m), 1371 (w), 1037 (s), 1035 (s), 993 (s), 902 (s), 601 (m) cm^{-1}.

2.3. Synthesis of $(C_3N_2H_{12})_4\{Co_3$ $[P_4Mo_6O_{26}(OH)_5]_2\}\cdot 5H_2O$ (**2**)

The preparation of compound **2** was similar to that of **1** except that 1,3-propanediamine (0.5 mL) was used instead of ethylenediamine (0.5 mL). Navy blue block crystals of **2** were filtered, washed with water, and dried at room temperature. The yield is 42% based on Co. Anal. Found (%): C, 4.59; H, 2.66; N, 3.38. Calcd. (%): C, 4.85; H, 2.31; N, 3.77. IR (KBr, pellet): 3423 (m), 3249 (m), 1629 (m), 1527 (w), 1085 (s), 1037 (s), 958 (s), 742 (m), 684 (m), 613 (w), 538 (m), 503 (m) cm^{-1} (Fig. S2).

Table 1
Crystal structure and refinement data for **1** and **2**.

	1	**2**
Empirical formula	$C_2H_{15}O_{12}N_2P_2CoMo$	$C_{12}H_{68}O_{67}N_8P_8Co_3Mo_{12}$
Formula weight (g/mol)	475.97	2972.56
λ (Å)	0.71073	0.71073
T (K)	273(2)	273(2)
Crystal dimensions (mm^3)	$0.20\times0.16\times0.10$	$0.20\times0.10\times0.06$
Crystal system	Triclinic	Monoclinic
Space group	P_{-1}	$P_{21/c}$
a (Å)	5.0504(11)	25.108(3)
b (Å)	7.4840(17)	12.3041(13)
c (Å)	9.138(2)	32.111(3)
α (deg)	72.543(3)	90.00
β (deg)	85.870(3)	127.454(6)
γ (deg)	70.711(2)	90.00
V ($Å^3$)	310.85(12)	7875.0(16)
Z	1	4
D_{calcd} (g/cm^{-3})	2.537	2.499
μ (mm^{-1})	2.667	2.734
$F(000)$	235	5708.0
θ range (deg)	3.02–28.27	2.45–28.30
Data/restraints/parameters	1506/0/100	18,878/180/969
R_{int}	0.0090	0.0582
Final R_1[a], wR_2[b] [$I>2\sigma(I)$]	0.0487, 0.1141	0.0548, 0.1259
Final R_1[a], wR_2[b] (all data)	0.0488, 0.1141	0.0927, 0.1471
Goodness-of-fit on F^2	1.000	1.000
Largest diff.	1.158/−2.166	4.200/−2.402

[a] $R_1=\sum||F_o|-|F_c||/\sum|F_o|$.
[b] $wR_2=\sum[w(F_o^2-F_c^2)^2]/\sum[w(F_o^2)^2]^{1/2}$.

2.4. X-ray crystallographic study

The structures of compounds **1** and **2** were determined by single crystal X-ray diffraction. Data were collected on a Bruker Apex-II CCD diffractometer with graphite-monochromated Mo$K\alpha$ radiation ($\lambda=0.71073$ Å) at 273/293 K. All of the structures were solved by the direct method and refined by the full-matrix least-squares method on F^2 using the *SHELXL*-97 software [34,35]. In the final refinements, all nonhydrogen atoms were refined anisotropically. For the compounds **1** and **2**, all of the H atoms attached to C atoms were generated geometrically. Crystallographic data and structure refinements for **1** and **2** are given in Table 1. Selected bond lengths for **1** and **2** are listed in Tables S1 and S2.

3. Results and discussion

3.1. Syntheses

Compounds **1** and **2** were synthesized under almost the same hydrothermal conditions except for using amines with different lengths. Currently, the hydrothermal synthesis techniques have proved to be invaluable for the synthesis of almost all kinds of recently important materials, in particular layered and porous materials [36–38]. In the field of POMs, a wide variety of molybdophosphates with transition-metal complexes (PMo–TMCs) have been successfully synthesized by directing of the organic amines under hydrothermal conditions [39–48]. Therefore, the introduction of hydrothermal techniques and direct use of organic amines as templates may produce a large number of new functional materials based on POMs [49–53]. However, the skeletons of polyoxoanions are difficult to template-directed synthesis in constructing PMo–TMCs under hydrothermal conditions, depending upon the reaction conditions, such as starting materials, temperature, pH, filling volume and stoichiometry. Among these factors, pH value and temperature were proved crucial for constructing the skeleton of polyoxoanions [15–23,49–53]. In all these

reactions, it is found that the $\{P_2Mo_5\}$-based composite compounds are generally isolated at 160 °C, while most $\{P_4Mo_6\}$-based compounds should be prepared above 180 °C. Further, both $\{P_2Mo_5\}$- and $\{P_4Mo_6\}$-based compounds can be synthesized in a wide range of pH values, while the $\{PMo_{12-x}TM_xO_{40}\}$-based compounds can only be isolated in a very narrow pH range of ca. 3.5–4. In addition, during the syntheses of PMo–TMCs, the use of protonated organic amines such as en may play the important templating and reductant role for the assembly of the polyoxoanions. Numerous successful experimental results from so-called "black-box" reactions (hydrothermal conditions) could suggest some preliminary synthetic experiences, which might be helpful for the future synthetic route.

By doing many trials, we found that en and pn were good candidates for target syntheses of PMo–TMCs. In this work, two layered cobalt–molybdenum phosphates **1** and **2** were synthesized with a mixture of $Na_2MoO_4 \cdot 2H_2O$, $2CoCO_3 \cdot 3Co(OH)_2 \cdot H_2O$, H_3PO_4, H_4EDTA and en/pn in water at 180 °C for 7 days. The initial pH value was controlled in the range of 3.7–3.8. If the reaction temperature is lower than 180 °C or the pH value is outside the range of 3.7–3.8, no crystals could be obtained. Our parallel experiments have indicated that the use of EDTA species was necessary for compounds, although it was not involved in the final structures. If no H_4EDTA was introduced into the reaction mixture, another $\{Mo_5P_2\}$-based composite compound was isolated, which is similar to the reports [40,44].

3.2. Structural description of compound **1**

The single-crystal X-ray analysis reveals that the asymmetric unit of compound **1** $(C_2N_2H_{10})$ $[HCo(H_2O)_2P_2MoO_{10}]$ consists of $[CoMoP_2]$ clusters and ethylenediamine cations (shown in Fig. 1). The structure of $[CoMoP_2]$ cluster anions is constructed from $\{CoO_4(H_2O)_2\}$ octahedra, $\{PO_4\}$ tetrahedra, and $\{MoO_6\}$ octahedra linked through sharing vertices (Fig. 1b). The geometric parameters of the cobalt–molybdenum phosphate framework show that the P(1)–O contacts in the range 1.501(4)–1.567(4) Å and Mo(1)–O contacts in the range 1.938(4)–1.992(4) Å.

Note that the geometry around the cobalt atom in compound **1** is a distorted elongated octahedron involving the four oxygen atoms(O(1)#4/ O(1)#6, O(5)/ O(5)#5) and two oxygen atoms(O(6)/ O(6)#5) from two coordinated water molecules. The distances of Co(1)–O(6)(2.154(4) Å) are longer than the distances of Co(1)–O(1)/O(5)(2.025(4)/2.083(4) Å). Therefore the environment of the Co(II) ion consists of four short in-plane bonds and two longer out-of-plane bonds giving rise to the usual "4+2" octahedral configuration.

Compound **1** exhibits a supramolecular layered framework in which prontonated ethylenediamine molecules lodge (shown in Fig. 2a). Its structure consists of $\{MoO_6\}$ octahedra, $\{CoO_6\}$ octahedra and $\{PO_4\}$ tetrahedra through sharing vertices. As shown in Fig. 2b, adjacent $\{CoO_4(H_2O)_2\}$ octahedra and $\{MoO_6\}$ octahedra are alternately connected in a corner-sharing mode to form the infinite one-dimensional linear chain structure along *b*-axis. And the neighboring 1D chains, are linked together in the corner sharing manner through adjacent $\{PO_4\}$ tetrahedra, giving rise to the formation of 2D layers parallel to the *ab*-plane. Note that compound **1** is a 2, 4-connected 2D framework with $(6^4 \cdot 8 \cdot 10)(6)$ topology (shown in Fig. 2c). In this simplification, the 2-connected nodes are Co centers, 4-connected ones are Mo centers. The distances between Co(1) and Mo(1) are 3.742 and 5.050 Å.

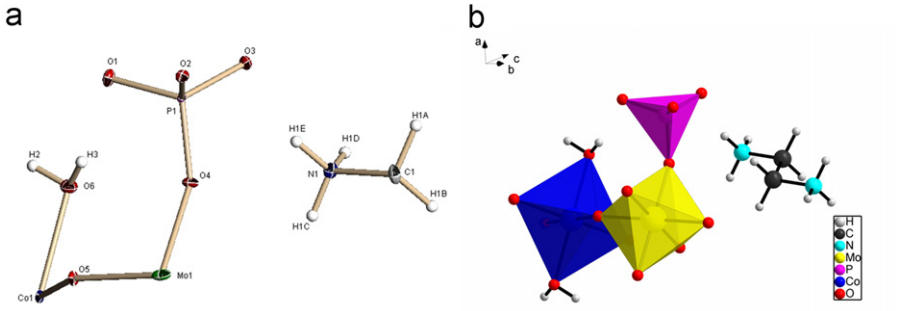

Fig. 1. (a) Molecular structure of compound **1**, with the atom labeling, showing displacement at the 30% ellipsoids probability level and (b) stick/polyhedral representation of the basic unit of compound **1**.

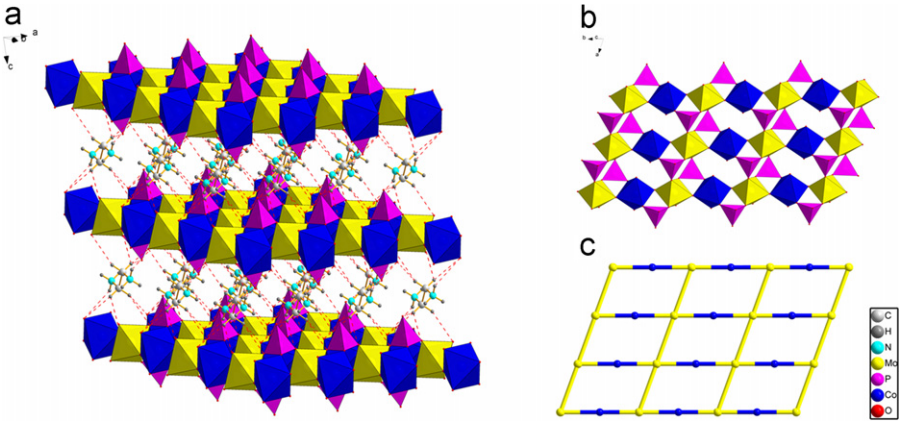

Fig. 2. (a) View of the H-bonding interactions between the surface O atoms of polyoxoanion and the H_2en groups in the supramolecular layered framework of compound **1**. The H-bonding interactions are indicated by red dotted lines. (b) View of 2D layered framework of compound **1** along *c*-axis. (c) View of the topology of compound **1** (the blue nodes symbolize the Co centers, and the yellow nodes symbolize Mo centers). (For interpretation of the references to color in this figure legend, the reader is referred to the web version of this article.)

Furthermore, a supramolecular structure is formed by H-bonding interactions between the neighboring layers and protonated H_2en ligands (shown in Fig. 2a). The protonated H_2en ligands are linked with neighboring metal-oxo clusters via N–H···O hydrogen bonds. The typical bond distances are N(1)–H(1D)···O(1) (2.900(7) Å), N(1)–H(1C)···O(3) (2.847(7) Å), N(1)–H(1D)···O(3) (3.048 (7) Å) and N(1)–H(1E)···O(3) (2.890(7) Å), respectively.

3.3. *Structural description of compound* **2**

The single-crystal X-ray analysis reveals that compound **2** consists of sandwich-shaped $[Co(Mo_6P_4)_2]$ clusters, cobalt cations, 1,3-propanediamine cations and lattice water molecules. As shown in Fig. 3, each octahedral Co^{2+} cation (Co(3)) links two $[P_4Mo_6]$ units together via six μ–O atoms (O(8), O(9), O(10), O(11), O(12) and O(13)) with Co(3)–O bond lengths of 2.135(5), 2.178(5), 2.135(5), 2.128(5), 2.177(5) and 2.151(5) Å, respectively. The Co(3)–O bond angles vary from 84.0(2) to 179.6(2)°.As a classical unit described by Meyer and Haushalter [39], each $[Mo_6P_4]$ unit is made up of six $\{MoO_6\}$ octahedra and four $\{PO_4\}$ tetrahedral. Six $\{MoO_6\}$ octahedra are coplanar and constitute a hexameric ring with alternating Mo–Mo (2.577–2.602 Å) bonds and non-bonding Mo–Mo contacts (3.483–3.500 Å). Four $\{PO_4\}$ tetrahedra are linked to the ring by sharing corners with one $\{PO_4\}$ group located on the center of the ring and the other three groups around its periphery. The P–O bond lengths are in the range of 1.511(6)–1.555(6) Å and O–P–O bond angles vary from 106.3(3)° to 112.8(3)°. The Mo–O distances are in the range of 1.671(6)–2.301(5) Å.

Compound **2** also exhibits a layered framework in which H_2pn molecules lodge (shown in Fig. 4a). The 2D layered structure of **2** is constructed from the sandwich-shaped $[Co(Mo_6P_4)_2]$ clusters linked by $\{CoO_4\}$ tetrahedra (Co(2)/Co(3)) *via* sharing corners(-shown in Fig. 4b). In each crystallographically identical $\{CoO_4\}$tetrahedron, two O atoms are from one its neighboring $[Mo_6P_4]$ unit, one from the central phosphate tetrahedron and the other from a peripheral hydrophosphate tetrahedron. The two remaining O atoms are shared with two other adjacent $[Co(Mo_6P_4)_2]$ units. Therefore, each tetrahedral Co site contacts four phosphate groups from three different $[Co(Mo_6P_4)_2]$ units and each $[Co(Mo_6P_4)_2]$ unit is in turn coordinated to six tetrahedral Co atoms, forming a 2D layer. The Co(1)–O bond lengths are in the range of 1.921(6)–1.982(5) Å and O–Co(1)–O bond angles vary from 97.0(2)° to 117.4(3)°. The Co(2)–O bond lengths are in the range of 1.926(6)–1.981(5) Å and O–Co(2)–O bond angles vary from 98.1(2)° to 118.2(3)°.

Compound **2** is a 3, 6-connected 2D framework with $(4^3)_2(4^6\cdot6^6\cdot8^3)$ topology (shown in Fig. 4c). In this simplification, the 3-connected nodes are tetrahedral Co centers, 6-connected ones are sandwich-shaped $[Co(Mo_6P_4)_2]$ clusters. The distances between tetrahedral Co and octahedral Co are 6.750, 6.752, 9.152, 9.164, 9.461 and 9.468 Å.

In compound **2**, the H_2pn ligands adopt two kinds of conformations: the "W"-type conformation and the "S"-type conformation (shown in Fig. 5a). The torsion angles in the "W"-type and "S"-type were analyzed by the PLATON software tool. The data are summarized in Table 2.

Different from compound **1**, there are two categories of cavities of the layered framework in compound **2** (shown in Fig. 4b). The formation of these two categories of cavities may ascribe to template effect of the protonated H_2pn ligands. Between the layers, the "W"-type

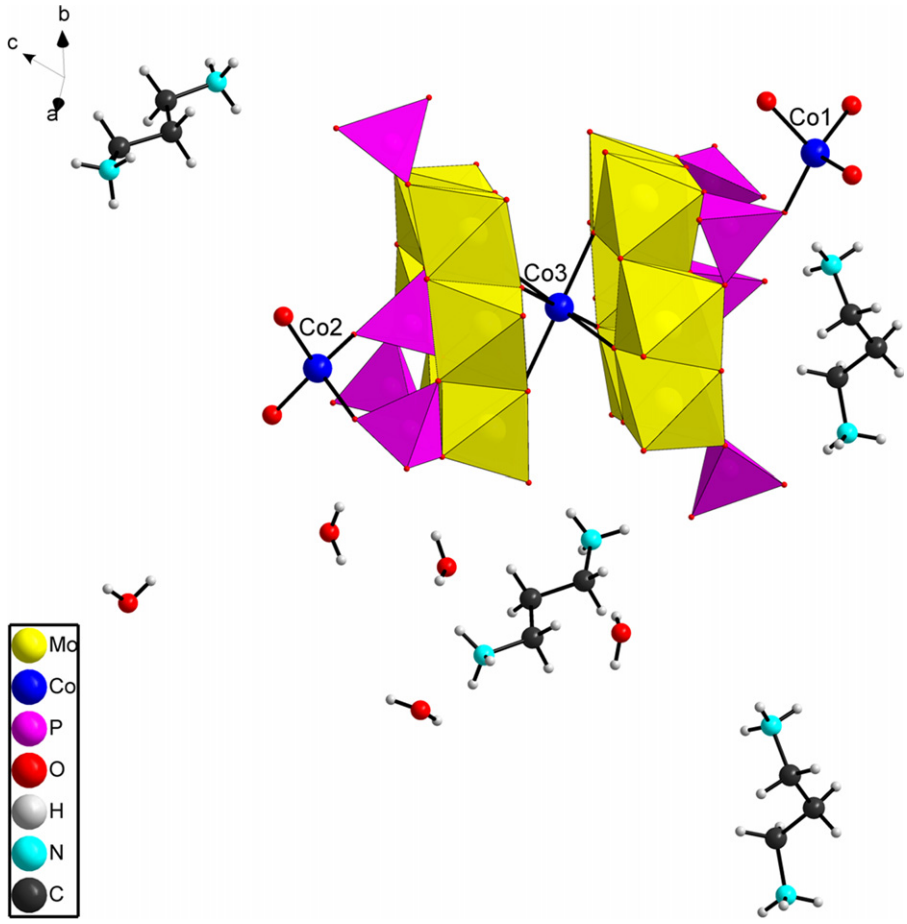

Fig. 3. Stick/polyhedral representation of the asymmetric unit of compound **2**.

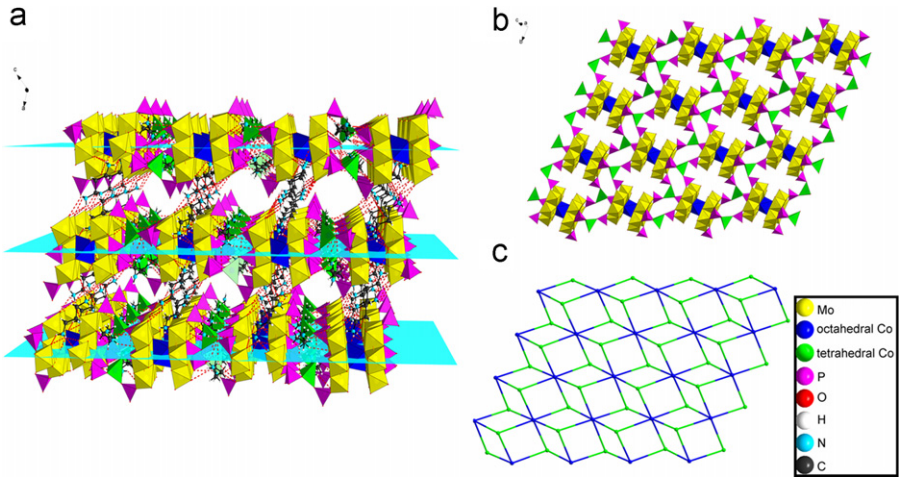

Fig. 4. (a) View of the H-bonding interactions between the surface O atoms of polyoxoanion and the H_2pn groups in the supramolecular layered framework of compound **2** along *b*-axis. The H-bonding interactions are indicated by red dotted lines. (b) View of 2D layered framework of compound **2**. (c) View of the topology of compound **2** (the blue nodes symbolize the sandwich-shaped $[Co(Mo_6P_4)_2]$ clusters, and the green nodes symbolize tetrahedral Co centers). (For interpretation of the references to color in this figure legend, the reader is referred to the web version of this article.)

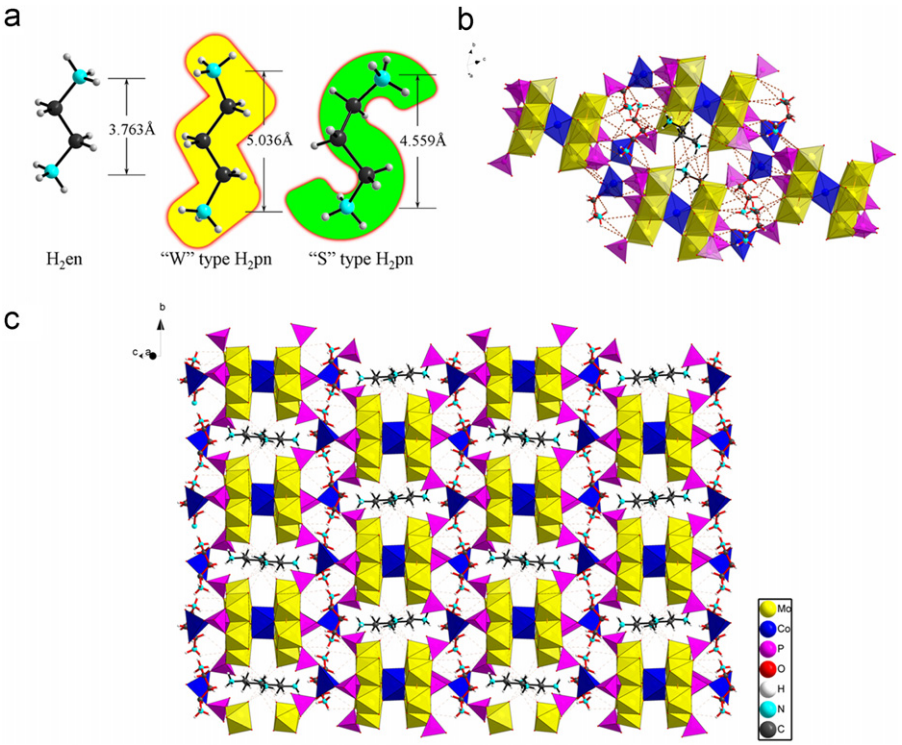

Fig. 5. (a) The different lengths of protonated organic amines used in the compounds **1** and **2**. (b) View of the H-bonding interactions(indicated by brown dotted lines) between the surface O atoms of metal-oxo clusters and two kinds of conformations of the H_2pn groups in compound **2**. (c) The protonated H_2pn ligands used to 'encapsulate' the inorganic building blocks in compound **2**. The bonds in "W"-type and "S"-type H_2pn ligands are presented in black and red, respectively. (For interpretation of the references to color in this figure legend, the reader is referred to the web version of this article.)

Table 2
Torsion/dihedral angles in compound **2.**

"W"-type conformation		**"S"-type conformation**	
C(6)···C(4)···C(5)···N(4)	172.1(14)	N(1)···C(1)···C(3)···C(2)	−120.7(16)
C(5)···C(4)···C(6)···N(3)	−177.6(11)	N(2)···C(2)···C(3)···C(1)	−80.0(18)
N(8)···C(10)···C(11)···C(12)	175.0(12)	N(5)···C(7)···C(8)···C(9)	−80(2)
C(10)···C(11)···C(12)···N(7)	−172.5(11)	C(7)···C(8)···C(9)···N(6)	−123.4(18)

H_2pn ligands adopt the fashion of upright not only to induce the formation of layered framework but also to direct the formation of the relatively bigger cavities (shown in Fig. 5). The bigger cavities are stacked in cruciform configurations, have Co(3)–Co(3) distances of 12.304 Å and Co(1)–Co(2) distances of 13.983 Å. The "W"-type H_2pn ligands are linked with neighboring metal-oxo clusters *via* N–H···O hydrogen bonds. The typical bond distances are N(3)–H(3D)···O(16) (3.001(13) Å), N(4)–H(4C)···O(40) (2.817(15) Å), N(7)–H(7D)···O(55) (2.855(16) Å) and N(8)–H(8C)···O(31) (2.831(12) Å), respectively. As shown in Figs. 4b and 5, the relatively smaller cavities are directed by "S"-type H_2pn ligands which adopt prostrate position in the framework. The smaller cavities are stacked in oval configurations with 8.219 Å × 5.261 Å. The "S"-type H_2pn ligands are linked with neighboring metal-oxo clusters *via* N–H···O hydrogen bonds. The typical bond distances are N(1)–H(1A)···O(30) (2.734(14) Å), N(2)–H(2A)···O(18) (2.824(12) Å), N(5)–H(5A)···O(25) (2.846(15) Å) and N(6)–H(6C)···O(33) (2.772(12) Å), respectively.

3.4. Influence of the organic amine on the structures of compounds **1** and **2**

In this work, through changing the lengths of amines, we have achieved the alternation of interlayer distances to observe the effect of protonated amines on the POM-based open-frameworks assembly (see Fig. 6). Compounds **1** and **2** were synthesized under identical reaction conditions except for the alternation of amines. It is clear that the protonated amines are the key factors influencing the structures and topologies of these compounds. Further, preliminary data do imply that the length, flexibility and conformation of the organic amines can influence the overall structure of the framework. The different lengths of protonated organic amines used in the compounds **1** and **2** are shown in Fig. 5(a). The H_2en ligands (ca. 3.763 Å) in compound **1** direct the [$CoMoP_2$] clusters neatly arranged, which results in layered framework with interlayer distances 8.713 Å. It acts as the structure-directing agent and also the charge balancing cation. In contrast with H_2en in compound **1**, the more flexible H_2pn ligands adopt both the "W"-type conformation (ca. 5.036 Å) and the "S"-type conformation (ca. 4.559 Å) in compound **2** in order to "encapsulate" the inorganic building blocks, therefore a supramolecular layered framework with interlayer distances 12.250 Å is obtained. The supramolecular framework may be best described as layers of polyoxoanions pillared by "W"-type H_2pn *via* intermolecular N–H···O hydrogen-bonding interactions. The result indicates that the conformation of the organic amines may influence the stacking mode of the inorganic building blocks in the crystal engineering of PMo–TMCs. The influence of the amines should be complex and synergic, including such factors as the discrepancies of sizes and conformation of the amines. This fact rationalizes that different lengths of amines could direct layers frameworks with different interlayer distances, which offers once more a practical evidence of target synthesis.

3.5. TG analyses

The thermal gravimetric (TG) analysis of compounds **1** and **2** were carried out from 25 to 800 °C. The TG measure (Fig. S3) shows one major weight loss. The weight loss of 19.85% in the temperature range of 220–570 °C are attributed to the loss of all H_2en organic ligands in the compound **1**. The value is close to the calculated value of 13.05% (~H_2en). The TG measure (Fig. S4) shows two major weight losses of compound **2**. The first weight loss of 3.02% in the temperature range of 70–150 °C corresponds to the release of all lattice water molecules, which is in accordance with the calculated one of 3.03% (~$5H_2O$). The second weight losses of 16.17% in the temperature range of 200–620 °C are attributed to the loss of all H_2pn ligands and the composition of water in the compound **2**. The value is close to the calculated value of 16.31% (~$4H_2$pn and $5H_2O$). The overall weight loss of 19.19% is in accordance with the calculated value of 19.34%. In order to identify the final decomposed products, we have analyzed the final decomposed products of compound **1** and **2** by XPS. The result indicates that there are only inorganic elements (Mo, P and Co) in the remaining decomposed products.

3.6. Magnetic susceptibility

The variable-temperature magnetic susceptibilities of **1** and **2** were measured between 2 and 300 K under 1 kOe magnetic field(shown in Fig. 7). The experimental susceptibilities were corrected for the diamagnetism of the constituent atoms (Pascal's tables) [54].

The plots of $\chi_m T$ and χ_m^{-1} vs. T of compound **1** was shown in Fig. 7a. At room temperature, the $\chi_m T$ product is 2.387 cm^3 K mol^{-1} (μ_{eff}= 4.37μ_B), smaller than the expected value (μ_{eff}=5.47μ_B) for one uncoupled Mo^V ions (S=1/2, g=2.00) and one uncoupled Co ions

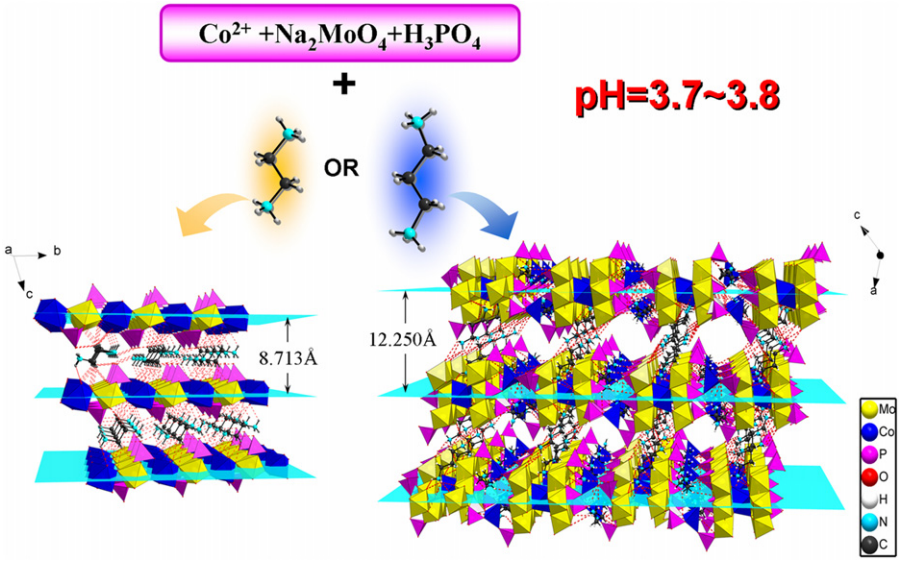

Fig. 6. Summary of the formation of layered structures with different interlayer distances, depending on the lengths of amine ligands used in the synthesis.

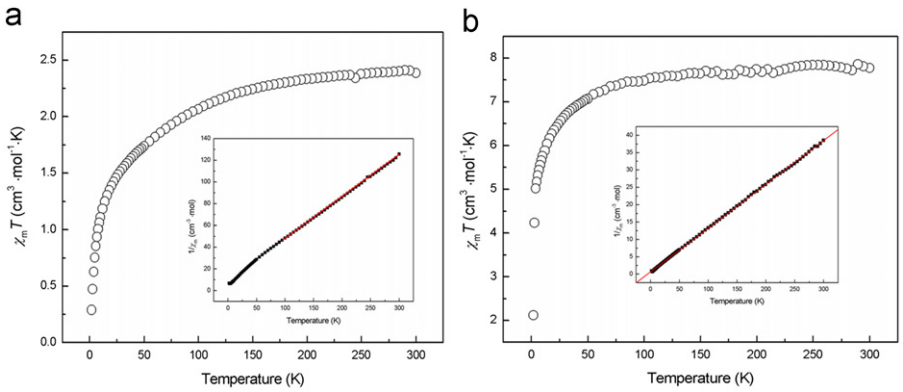

Fig. 7. $\chi_m T$ vs. T curve of compounds 1(a) and 2(b) from 2 to 300 K for at $H=1$ kOe (inset: χ_m^{-1} vs. T curve.The red line is the best fit with Curie–Weiss law.) (For interpretation of the references to color in this figure legend, the reader is referred to the web version of this article.)

($S=3/2$) taking into account an g-value of 2.68 [55]. On cooling, the $\chi_m T$ value decreases continuously to a minimum of 0.289 cm^3 K mol^{-1} at 2 K, suggesting a dominant antiferromagnetic exchange interaction. The χ_m^{-1} vs. T plot can be fitted by the Curie–Weiss law above 50 K with $C=2.626$ cm^3 K mol^{-1} and $\theta=-26.2$ K, respectively. The negative Weiss constant (θ) suggests the presence of antiferromagnetic interactions between the metal cations in compound **1**.

The thermal variations of $\chi_m T$ and χ_m^{-1}vs. T of compound **2** are shown in Fig. 7b. At room temperature, the $\chi_m T$ product is 7.777 cm^3 K mol^{-1} ($\mu_{eff}=7.892\mu_B$), smaller than the expected value ($\mu_{eff}=8.989\mu_B$) for three uncoupled Co^{2+} ions ($S=3/2$, assuming $g=2.68$ for Co^{2+}) [56]. Although valence states of Mo atoms are +5, but owing to formation of Mo–Mo metal bonds thus they have no contribution to magnetism of compound **2** [30]. The magnetic data of compound **2** obey Curie–Weiss law and give value of Curie constant $C=7.928$ cm^3 K mol^{-1} and $\theta=-5.065$ K, showing characteristic of an antiferromagnetic interaction.

Unfortunately, it is too difficult to fit the experimental magnetic data of this compound using a suitable theoretical model, and further studies on magnetic properties of similar systems are ongoing in our laboratory.

4. Conclusions

In this paper, two organically templated cobalt–molybdenum phosphates were synthesized under hydrothermal conditions, both of which contain novel layer topologies. During the synthesis of PMo–TMCs, the use of protonated organic amines might play the important templating role for the assembly of the polyoxoanions. Our investigations have found that the interlayer distances of the title compounds can be changed by using organic amine with different lengths under hydrothermal environment, such as ethylenediamine and 1,3-propanediamine. Interestingly, the H_2pn in compound **2** adopt both the "W"-type conformation and the "S"-type conformation to form a layered framework with two categories of cavities. The results show that the conformation of the organic amines may influence the stacking mode of the inorganic building blocks in the crystal engineering of PMo–TMCs. This work implies that the chain lengths and conformation of the organic amines can influence the overall supramolecular framework of the PMo–TMCs, which offers once more a practical evidence of target synthesis. More efforts will focus on the PMo–TMCs reaction system so as to explore the possible effect of different amines in the engineering of POM clusters under hydrothermal environment and their multi-functionalities.

Supplementary material

Crystallographic data in CIF format. CCDC reference numbers: 771428 for compound **1**, 771429 for compound **2**. These data can be obtained free of charge from The Cambridge Crystallographic Data Centre via www.ccdc.cam.ac.uk/data_request/cif.

Acknowledgments

This work is supported by the National Natural Science Foundation of China (Grants Nos. 20671026, 20971032 and 20901031), the Study Technological Innovation Project Special Foundation of Harbin (Grant No. 2009RFXXG202), the Science and Technology Project of Jiamusi University (L2009-105), and Natural Science Foundation of Heilongjiang Province of China (Grants Nos. B200901 and B200916).

Appendix A. Supplementary material

Supplementary data associated with this article can be found in the online version at doi:10.1016/j.jssc.2010.12.010.

References

[1] G. Xu, G.C. Guo, M.S. Wang, Z.J. Zhang, W.T. Chen, J.S. Huang, Angew. Chem. Int. Ed. 46 (2007) 3249.
[2] W.H. Bi, N. Louvain, N. Mercier, J. Luc, I. Rau, F. Kajzar, B. Sahraoui, Adv. Mater. 20 (2008) 1013.
[3] C.R. Kagan, D.B. Mitzi, C.C. Dimitrakopoulos, Science 286 (1999) 945.
[4] A.K. Cheetham, G. Férey, T. Loiseau, Angew. Chem. Int. Ed. 38 (1999) 3268.
[5] K. Egeblad, C.H. Christensen, M. Kustova, C.H. Christensen, Chem. Mater. 20 (2008) 946.
[6] J.M. Thomas, J. Klinowski, Angew. Chem. Int. Ed. 46 (2007) 7160.
[7] S.H. Feng, R.R. Xu, Acc. Chem. Res. 34 (2001) 239.
[8] J.H. Yu, R.R. Xu, Acc. Chem. Res. 36 (2003) 481.
[9] X.M. Zhang, M.L. Tong, X.M. Chen, Angew. Chem. Int. Ed. 41 (2002) 1029.
[10] C.J. Janiak, Chem. Soc. Dalton Trans. (2003) 2781.
[11] J.R. Galán-Mascarós, C. Gimenez-Saiz, S. Triki, C.J. Goméz-Garcia, E. Coronado, L. Ouahab, Angew. Chem. Int. Ed. 34 (1995) 1460.
[12] J. Tao, Y. Zhang, M.L. Tong, X.M. Chen, T. Yuen, C.L. Lin, X.Y. Huang, J. Li, Chem. Commun. (2002) 1342.
[13] X.B. Cui, J.Q. Xu, H. Meng, S.T. Zheng, G.Y. Yang, Inorg. Chem. 43 (2004) 8005.
[14] J.P. Wang, P.T. Ma, J.Y. Niu, Inorg. Chem. Commun. 9 (2006) 1049.
[15] C. Streb, D.L. Long, Leroy Cronin, Chem. Commun. (2007) 471.
[16] W.J. Chang, Y.C. Jiang, S.L. Wang, K.H. Lii, Inorg. Chem. 45 (2006) 6586.
[17] Y.H. Sun, X.B. Cui, J.Q. Xu, L. Ye, Y. Li, J. Lu, H. Ding, H.Y. Bie, J. Solid State Chem. 177 (2004) 1811.
[18] Y. Ma, Y.G. Li, E.B. Wang, Y. Lu, X.X. Xu, X.L. Bai, Transition Met. Chem. 31 (2006) 262.
[19] C. Streb, D.L. Long, L. Cronin, Cryst. Eng. Commun. 8 (2006) 629.

[20] M.I. Khan, L.M. Meyer, R.C. Haushalter, A.L. Schweitzer, J. Zubieta, J.L. Dye, Chem. Mater. 8 (1996) 43.
[21] C.L. Pan, J.Q. Xu, G.H. Li, X.B. Cui, Y. Le, G.D. Yang, Dalton Trans. (2003) 517.
[22] Y. Ishii, Y. Takenaka, K. Konishi, Angew. Chem. Int. Ed. 43 (2004) 2702.
[23] H.Y. An, E.B. Wang, D.R. Xiao, Y.G. Li, Z.M. Su, L. Xu, Angew. Chem. Int. Ed. 45 (2006) 904.
[24] G. Férey, Chem. Mater. 13 (2001) 3084.
[25] D.L. Long, P. Kögerler, L.J. Farrugia, L. Cronin, Dalton Trans. (2005) 1372.
[26] H. Abbas, A.L. Pickering, D.L. Long, P. Kögerler, L. Cronin, Chem. Eur. J. 11 (2005) 1071.
[27] D.L. Long, H. Abbas, P. Kögerler, L. Cronin, Angew. Chem. Int. Ed. 44 (2005) 3415.
[28] D.L. Long, P. Kögerler, L. Cronin, Angew. Chem. Int. Ed. 43 (2004) 1817.
[29] D.L. Long, P. Kögerler, L.J. Farrugia, L. Cronin, Angew. Chem. Int. Ed. 42 (2003) 4180.
[30] Z.H. Yi, X.Y. Yu, W.J. Xia, L.Y. Zhao, C. Yang, Q. Chen, X.L. Wang, X.Z. Xu, X. Zhang, Cryst. Eng. Commun. 12 (2010) 242.
[31] X. Zhang, Z.H. Yi, L.Y. Zhao, Q. Chen, X.L. Wang, J.Q. Xu, W.J. Xia, C. Yang, Cryst. Eng. Commun. 12 (2010) 595.
[32] Y.N. Zhang, B.B. Zhou, Y.G. Li, Z.H. Su, Z.F. Zhao, Dalton Trans. (2009) 9446.
[33] Y.N. Zhang, B.B. Zhou, Q.Q. Sha, Z.H. Su, H. Liu, Inorg. Chem. Commun. 13 (2010) 550.
[34] G.M. Sheldrick, SHELXS97, Program for X-ray Crystal Structure Refinement, University of Göttingen: Göttingen, Germany, 1997.
[35] G.M. Sheldrick, SHELXS97, Program for X-ray Crystal Structure Solution, University of Göttingen, Göttingen, Germany, 1997.
[36] D. Wu, S. Lin, E. Tang, G.Y. Yan, C. R. Chim. 11 (2008) 152.
[37] X.M. Zhang, J.J. Hou, W.X. Zhang, X.M. Chen, Inorg. Chem. 45 (2006) 8120.
[38] L.M. Dai, W.S. You, Y.G. Li, E.B. Wang, C.Y. Huang, Chem. Commun. (2009) 2721.
[39] L.A. Meyer, R.C. Haushalter, Inorg. Chem. 32 (1993) 1579.
[40] J.J. Lu, Y. Xu, N.K. Goh, L.S. Chia, Chem. Commun. (1998) 1709.
[41] U. Kortz, Inorg. Chem. 39 (2000) 623.
[42] C.D. Peloux, P. Mialane, A. Dolbecq, J. Marrot, F. Varret, F. Secheresse, Solid State Sci. 6 (2004) 719.
[43] L.Y. Duan, F.C. Liu, X.L. Wang, E.B. Wang, C. Qin, Y.G. Li, X.L. Wang, C.W. Hu, J. Mol. Struct. 705 (2004) 15.
[44] H.X. Guo, S.X. Liu, Inorg. Chem. Commun. 7 (2004) 1217.
[45] X. He, P. Zhang, T.Y. Song, Z.C. Mu, J.H. Yu, Y. Wang, J.N. Xu, Polyhedron 23 (2004) 2153.
[46] W.B. Yang, C.Z. Lu, C.D. Wu, S.F. Lu, D.M. Wu, H.H. Zhuang, J. Cluster Sci. 13 (2002) 43.
[47] J.R.G. Mascaros, C. Marti-Gastaldo, Polyhedron 26 (2007) 626.
[48] X.Z. Liu, B.Z. Lin, L.W. He, X.F. Huang, Y.L. Chen, J. Mol. Struct. 877 (2008) 72.
[49] P.J. Hagrman, D. Hagrman, J. Zubieta, Angew. Chem. Int. Ed. 38 (1999) 2638.
[50] Y. Lu, Y.G. Li, E.B. Wang, J. Lü, L. Xu, R. Clérac, Eur. J. Inorg. Chem. 7 (2005) 1239.
[51] C. Peloux, A. Dolbecq, P. Mialane, J. Marrot, E. Rivière, F. Sécheresse, Angew. Chem. Int. Ed. 40 (2001) 2455.
[52] J.W. Zhao, C.M. Wang, J. Zhang, S.T. Zheng, G.Y. Yang, Chem. Eur. J. 14 (2008) 9223.
[53] S.T. Zheng, J. Zhang, G.Y. Yang, Angew. Chem. Int. Ed. 47 (2008) 3909.
[54] E.A. Boudreaux, J.N. Mulay, Theory and Application of Molecular Paramagnetism, John Wiley & Sons, New York, 1976.
[55] C.L. Pan, J.F. Song, J.Q. Xu, G.H. Li, L. Ye, T.G. Wang, Inorg. Chem. Commun. 6 (2003) 535.
[56] C.M. Liu, D.Q. Zhang, M. Xiong, D.B. Zhu, Chem. Commun. (2002) 1416.